Proceedings of the
Annual Stability Conference
Structural Stability Research Council
Nashville, Tennessee, March 24-27, 2015

Elastic Stability of uniform and non-uniform members with arbitrary boundary conditions and intermediate lateral restraints

André Beyer[1], Yvan Galéa[2], Alain Bureau[3], Nicolas Boissonnade[4]

Abstract
The elastic stability of tapered beams has been investigated many times in the past. However, most of these studies consider beams subjected to bending moments only and therefore they do not consider the influence of axial force on the stability of the member. Consequently, flexural and torsional buckling modes under pure compression or combined compression and bending cannot be represented.
The present paper presents – to the authors' knowledge – the first freely available program, *LTBeamN*, that allows designers to assess the-out-of plane elastic stability of beam columns considering the combined influences of the taper of the beam, intermediate lateral restraints and interaction of axial force and bending moments.
First, the theoretical background of *LTBeamN* is presented. The linear and geometrical element stiffness matrices of the beam elements are derived on the basis of the energy method. In particular, the influence of the taper on the torsional behavior of the beam is pointed out.
Numerical examples are then given to illustrate and validate the calculation of the critical load amplifier. Finally, a practical example shows how *LTBeamN* can simplify the verification of a tapered member with intermediate lateral restraints, by means of the global slenderness concept as proposed by the European standard Eurocode 3 (CEN 2005).

1. Introduction

The design of beam-columns is usually done using formulas that have been calibrated on the basis of physical tests and numerical simulations on single span uniform beams with fork end conditions and without any intermediate lateral restraint. However, members in actual structures often possess lateral restraints and may be non-uniform. A typical example of such members is the rafter of industrial buildings. It is questionable, if the standard design formulas can be used in these cases. That is why, the European standard Eurocode 3 (CEN 2005) proposes the so called "general method for lateral and lateral torsional buckling of structural components". This method is based on the global non dimensional slenderness of the member as defined by Eq. (1).

[1] Research Engineer, CTICM, <abeyer@cticm.com>
[2] Former head of steel research department, CTICM, < ygalea@cticm.com >
[3] Head of steel research department, CTICM, <abureau@cticm.com>
[4] Professor, University of Applied Sciences of Western Switzerland, <nicolas.boissonnade@hefr.ch>

$$\bar{\lambda}_{op} = \sqrt{\frac{\alpha_{ult,k}}{\alpha_{cr,op}}} \tag{1}$$

where $\alpha_{ult,k}$ is the minimum load amplifier of the design loads to reach the characteristic resistance of the most critical cross section of the member considering in plane behavior and accounting for in plane second order effects and in plane imperfections, while $\alpha_{cr,op}$ is the minimum amplifier for the design loads to reach the elastic critical resistance of the member with regards to out-of-plane instability, i.e. lateral or lateral torsional buckling.

The first factor can be determined easily on the basis of the internal forces and the section resistance of the member at a given point along the length. Yet, in presence of intermediate lateral restraints and/or non-uniform members, the determination of the critical load amplification factor $\alpha_{cr,op}$ is not simple. Analytical methods for beams with intermediate lateral restraints have been proposed in the 70's and 80's for example by (Nethercot 1976) and (Kitipornchai 1982). Both propose iterative methods for beams with rigid intermediate torsional restraints giving satisfactory results. Though, because of the iterative character of these methods their application is very limited in today's practice.

Additionally, these methods are limited to members with rigid local intermediate restraints; consequently they cannot be used for members possessing an elastic continuous restraint as created for example by roof sheeting.

In order to enable the application of the "general method" engineers are therefore in need of a tool that determines the critical load amplification factor simply and reliably. In case of uniform double symmetric beams with intermediate lateral restraints, some commercial and non-commercial software exist to do so, as for example *LTBeam* developed by the second author (Galéa 2003). However, in the case of non-uniform members, most software require the beam to be modelled by finite shell elements. This longsome and delicate procedure might be used for research but is not reasonable in practice.

Over the time, the behavior of tapered beams has been studied by (Wilde 1968), (Kitipornchai 1972) and (Kitipornchai 1975), (Bradford 1988), (Ronagh 2000), (Boissonnade 2002), (Andrade 2007) and (Asgarian 2013) among others. This long and, however, incomplete list shows that the subject of tapered members has not lost its interest up to present days. All the aforementioned authors have demonstrated the difference in the torsional behavior between uniform and non-uniform members, in a more or less similar way. However, even as the research on tapered members began nearly 50 years ago, no freely available tool has been published for the calculation of the critical load amplification factor for tapered beams. This lack has been overcome with the development of *LTBeamN* (LTBeamN 2013), a free numerical tool for the calculation of critical load amplification factor $\alpha_{cr,op}$. Fig. 1 shows a screen shot of the Graphical User Interface of *LTBeamN*.

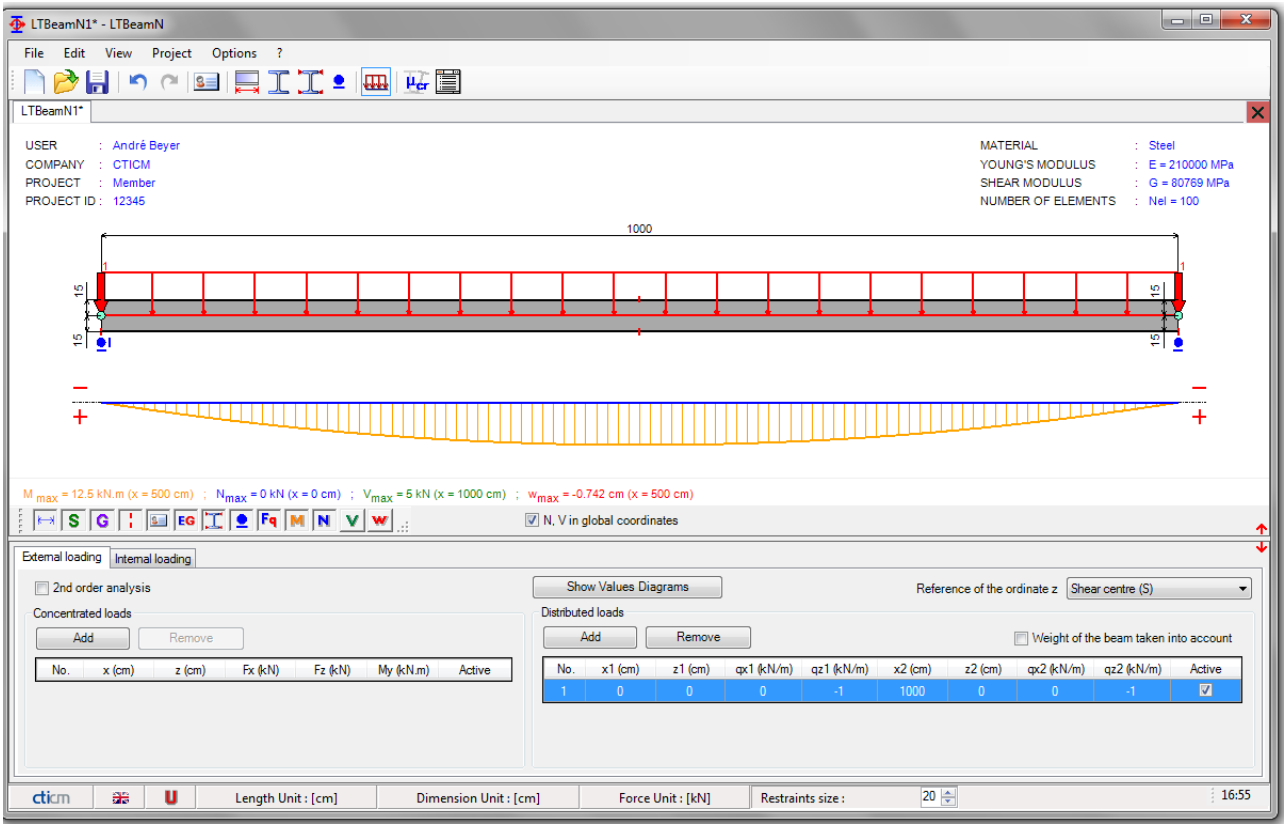

Figure 1: Graphical User Interface of LTBeamN

The calculation is based on finite beam elements considering the effects of the non-uniformity of the beam, intermediate lateral restraints and interaction of axial force and bending moments. This paper presents the derivation of the element stiffness matrices (§3 of this paper). The validation of *LTBeamN* is illustrated on the basis of some examples (§4 of this paper) and finally the use of *LTBeamN* for the design of non-uniform members with intermediate lateral restraints is explained for a practical case (§5 of this paper).

2. Sign Convention and Limitations

In the following, the derivation of the element stiffness matrix is based on the co-ordinate system shown in Fig. 2. The co-ordinate system is referred to the centroid *G* of a given cross section.

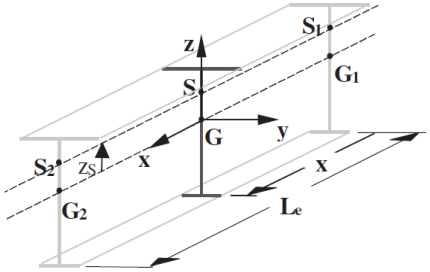

Figure 2: Coordinate system

Hereafter, it is considered that deformations in the positive direction of the axes *x*, *y* and *z* are positive. Bending moments compressing the upper fibers of the cross section are assumed to be positive as well as compressive axial forces.

Also, only the widely used I/wide flange open cross sections are considered. These cross sections can be mono- or double-symmetric.

As stated above, the critical load amplification factor used in Eq. (1) should be calculated with regard to lateral (out-of-plane) and lateral-torsional buckling (CEN 2005). In-plane buckling should not be accounted for. Consequently, the beam element degrees of freedom considered for the element stiffness matrix are the lateral displacement v, the out-of-plane curvature $v_{,x}$[5], the torsional rotation θ, and the warping deformation $\theta_{,x}$.

3. Derivation of the element stiffness matrix

3.1 Methodology adopted

The element stiffness matrix is derived on the basis of the energy method which states that the total potential energy of a member is the sum of the internal energy and the work of the external forces. In case of a linear elastic material, the internal energy can be expressed with Eq. (2):

$$\Pi_i = \int \frac{1}{2} E\varepsilon_{xx,L}^2 + E\varepsilon_{xx,L}\varepsilon_{xx,NL} dV + \int 2G\left(\varepsilon_{xy,L}^2 + \varepsilon_{xy,L}^2\right) + 2G\left(\varepsilon_{xy,L}\varepsilon_{xy,NL} + \varepsilon_{xz,L}\varepsilon_{xz,NL}\right) dV \tag{2}$$

where Π_i is the internal potential energy, E is the Young's modulus, G is the shear modulus, $\varepsilon_{xx,L}$ and $\varepsilon_{xx,NL}$ are the linear and nonlinear part of the normal strain along x axis, $\varepsilon_{xy,L}$, $\varepsilon_{xz,L}$, $\varepsilon_{xy,NL}$ and $\varepsilon_{xz,NL}$ are the linear and nonlinear parts of the associated shear strains and V is the volume. The work of the external forces can be expressed with Eq. (3).

$$\Pi_e = \sum \int q_z W dx + \sum F_z W \tag{3}$$

where Π_e is the external work, q_z is a distributed vertical load, F_z is a vertical point load and W is vertical displacement of the load.
The global stiffness matrix is then derived by the condition:

$$\frac{\partial\partial\left(\Pi_i - \Pi_e\right)}{\partial a_i \partial a_j} = 0 \tag{4}$$

where a_i and a_j are the degrees of freedom considered. Generally, the stiffness matrix is divided in a so called linear stiffness matrix K_0, depending only on cross section constants and a so called geometric stiffness matrix K_σ, depending on the applied loads and the internal forces. On the basis of the linear and the geometric stiffness matrix, the critical load amplification factor is calculated with Eq. (5).

[5] $A_{,x}$ stands for the first derivate of the function A with respect to x.

$$K_0 - \alpha_{cr,op} K_\sigma = 0 \tag{5}$$

3.2 Internal energy of the member

In order to express the elastic strains of Eq. (2), an appropriate displacement field has to be chosen. Here the linearized displacement field of Eq. (6) is adopted.

$$\begin{aligned} U &= u - yv_{,x} - zw_{,x} - \omega_G \theta_{,x} \\ V &= v - z\theta \\ W &= w + y\theta \end{aligned} \tag{6}$$

where U is the longitudinal displacement of a point P of the section, V is the lateral displacement of P, W is the vertical displacement of P, u is the longitudinal displacement of the centroid G of the section, v is the lateral displacement of G, w is the vertical displacement of G, θ is the rotation of the section about its longitudinal axis, y is the lateral distance between G and P, z is the vertical distance between G and P, ω_G is the warping function at point P with reference to G. It is now considered that the torsional rotation θ acts about the shear center of the section. Hence, the displacement field of Eq. (6) should be expressed with reference to C. In order to do so, Eq. (7) gives the expression of the displacement at the centroid as a function of the displacements of the shear center:

$$\begin{aligned} v &= v_c + z_c \theta \\ w &= w_c - y_c \theta \\ \omega_G &= \omega_c + y_c z - z_c y \end{aligned} \tag{7}$$

Introducing (7) into (6), the displacement field with reference to the shear center of the section is obtained.

$$\begin{aligned} U &= u - y\left(v_c + z_c\theta\right)_{,x} - z\left(w_c - y_c\theta\right)_{,x} - \left(\omega_c + y_c z - z_c y\right)\theta_{,x} \\ V &= v - \left(z - z_c\right)\theta \\ W &= w + \left(y + y_c\right)\theta \end{aligned} \tag{8}$$

It was reported for example in (Boissonnade 2002) that for non-uniform members the general expression of the strains can be reasonably approximated by:

$$\begin{aligned} \varepsilon_{xx,L} &= U_{,x} + y_{,x}V_{,x} + z_{,x}W_{,x} & \varepsilon_{xx,NL} &= \frac{1}{2}\left(U_{,x}^2 + V_{,x}^2 + W_{,x}^2\right) \\ \varepsilon_{xz,L} &= \frac{1}{2}\left(U_{,z} + W_{,x} + y_{,x}V_{,z}\right) & \varepsilon_{xz,NL} &= \frac{1}{2}\left(U_{,x}U_{,z} + V_{,x}V_{,z}\right) \\ \varepsilon_{xy,L} &= \frac{1}{2}\left(U_{,y} + V_{,x} + z_{,x}W_{,y}\right) & \varepsilon_{xy,L} &= \frac{1}{2}\left(U_{,x}U_{,y} + W_{,x}W_{,y}\right) \end{aligned} \tag{9}$$

One can notice that Eq. (9) differs from traditional expressions used for uniform members given in Eq. (10) (Galéa 2003), with respect to $y_{,x}$ and $z_{,x}$ terms:

$$\varepsilon_{xx,L} = U_{,x} \qquad \varepsilon_{xx,NL} = \frac{1}{2}\left(U_{,x}^2 + V_{,x}^2 + W_{,x}^2\right)$$
$$\varepsilon_{xz,L} = \frac{1}{2}\left(U_{,z} + W_{,x}\right) \qquad \varepsilon_{xz,NL} = \frac{1}{2}\left(U_{,x}U_{,z} + V_{,x}V_{,z}\right) \tag{10}$$
$$\varepsilon_{xy,L} = \frac{1}{2}\left(U_{,y} + V_{,x}\right) \qquad \varepsilon_{xy,L} = \frac{1}{2}\left(U_{,x}U_{,y} + W_{,x}W_{,y}\right)$$

As for non-uniform members, the derivation of the co-ordinates *y* and *z* of a point *P* of the section may be a function of its longitudinal position their derivatives with respect to *x* must be kept in the expression of the strains. For double-symmetric I sections this fact can be explained regarding Fig. 3. It can be seen that the vertical position of the flanges at the origin is $z(0) = \pm g_O$ whereas the position of the flanges at the extremity is $z(dx) = \pm g_E = \pm(g_O + dz)$. Consequently, the derivative $z_{,x}$ is not equal to 0. The same may be true for the derivative of the position y with respect to x for a general non-uniform member (for example C-section with varying flange width).

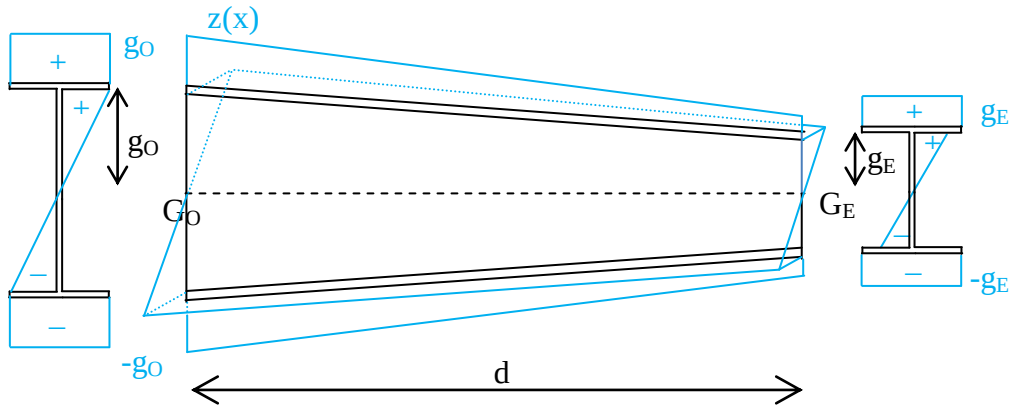

Figure 3: Vertical coordinate z for a non-uniform I-section

Introducing the displacement field given in Eq. (8) in the expressions of the strains given in Eq. (10) and solving the derivations lead to the following expressions of the total strains:

$$\begin{aligned}
&E_{xx} = \varepsilon_{xx,L} + \varepsilon_{xx,NL} = \\
&\left(u_{,x} - yv_{c,xx} - zw_{c,xx} - \omega_c\theta_{,xx} - \left(\omega_{c,x} + yz_{c,x} - zy_{c,x} + y_{,x}(z - z_c) - z_{,x}(y - y_c)\right)\theta_{,x}\right) + \\
&\frac{1}{2}\left(\begin{aligned}&\left(u_{,x} - yv_{c,xx} - zw_{c,xx} - \omega_c\theta_{,xx} - \left(\omega_{c,x} + yz_{c,x} - zy_{c,x} + y_{,x}(z - z_c) - z_{,x}(y - y_c)\right)\theta_{,x}\right)^2 \\ &+ \left(v_{c,x} - (z - z_c)\theta_{,x} - (z_{,x} - z_{c,x})\theta\right)^2 + \left(w_{c,x} + (y - y_c)\theta_{,x} + (y_{,x} - y_{c,x})\theta\right)^2\end{aligned}\right)
\end{aligned} \tag{11}$$

$$2E_{xz} = 2\left(\varepsilon_{xz,L} + \varepsilon_{xz,NL}\right) = \left(-\omega_{c,z}\theta_{,x} + (y - y_c)\theta_{,x}\right) + \left(-\theta v_{c,x} + \theta^2(z_{,x} - z_{c,x}) + \theta\theta_{,x}(z - z_c)\right)$$

$$2E_{xy} = 2\left(\varepsilon_{xy,L} + \varepsilon_{xy,NL}\right) = \left(-\omega_{c,y}\theta_{,x} - (z - z_c)\theta_{,x}\right) + \left(\theta w_{c,x} + \theta^2(y_{,x} - y_{c,x}) + \theta\theta_{,x}(y - y_c)\right)$$

Boissonnade showed that for regularly web-tapered beams the term $\omega_{c,x} + yz_{c,x} + zy_{c,x} + y_{,x}(z-z_c) - z_{,x}(y-y_c)$ is equal to $2\omega_{c,x}$ (Boissonnade 2002). Introducing this simplification in Eq. (11) gives a new expression for the normal strain in the x direction:

$$
\begin{aligned}
&\mathrm{E}_{xx} = \left(u_{,x} - yv_{c,xx} - zw_{c,xx} - \omega_c\theta_{,xx} - 2\omega_{c,x}\theta_{,x}\right) + \\
&\frac{1}{2}\left(\begin{aligned}&\left(u_{,x} - yv_{c,xx} - zw_{c,xx} - \omega_c\theta_{,xx} - 2\omega_{c,x}\theta_{,x}\right)^2 \\ &+\left(v_{c,x} - (z - z_c)\theta_{,x} - (z_{,x} - z_{c,x})\theta\right)^2 + \left(w_{c,x} + (y - y_c)\theta_{,x} + (y_{,x} - y_{c,x})\theta\right)^2\end{aligned}\right)
\end{aligned}
\tag{12}
$$

On the basis of the expressions for normal and shear strains, the internal energy of the member can be determined, leading to Eq. (13)[6]:

$$
\begin{aligned}
\Pi_i &= \frac{1}{2}\int EI_z v_{c,xx}^2 + EI_w\theta_{,xx}^2 + GI_t\theta_{,x}^2 + EI_\psi\theta_{,x}^2 + 2EI_{w\psi}\theta_{,x}\theta_{,xx} + 2EI_{y\psi}v_{c,xx}\theta_{,x}dx \\
&+ \frac{1}{2}\int N\left(v_{c,x}^2 + r_{yz}^2\theta_{,x}^2 + 2z_c v_{c,x}\theta_{,x} - r_{z,x}^2 v_{c,x}\theta + r_{yz,x2}^2\theta^2 + r_{yz,x}^2\theta\theta_{,x}\right)dx \\
&+ \int M_y\left(v_{c,x}\theta_{,x} - \beta_z\theta_{,x}^2 - \beta_{z,x2}\theta^2 - \beta_{z,x}\theta\theta_{,x} + \xi_{z.zx}v_{c,x}\theta\right)dx \\
&+ \int V_z\left(-v_{c,x}\theta + \frac{1}{2}r_{z,x}\theta^2\right)dx
\end{aligned}
\tag{13}
$$

where E is the Young's modulus of steel, G is the shear modulus of steel, N is the internal axial force, M_y is the bending moment, V_z is the shear force, I_z moment of inertia about the z-axis, I_w is the warping constant, I_t is the torsional constant, r_{yz} is the polar radius of gyration about the shear center, β_z is the Wagner coefficient for asymmetry about the y axis and I_ψ, $I_{w\psi}$, $I_{y\psi}$, $r_{z,x}$,$r_{y,x2}$, $r_{yz,x}$, $\beta_{z,x}$, $\beta_{z,x2}$, $\xi_{z,zx}$ are supplementary cross section constants associated with the taper of the beam. They are defined in Appendix A of this paper. It can be easily seen that expression (13) is much more complex than the corresponding expression of the internal energy of a uniform member given in Eq. (14) (Galéa 2003):

$$
\begin{aligned}
\Pi_i &= \frac{1}{2}\int EI_z v_{c,xx}^2 + EI_w\theta_{,xx}^2 + GI_t\theta_{,x}^2 dx \\
&+ \frac{1}{2}\int N\left(v_{c,x}^2 + r_{yz}^2\theta_{,x}^2 + 2z_c v_{c,x}\theta_x\right)dx + \int M_y\left(v_{c,x}\theta_{,x} - \beta_z\theta_{,x}^2\right)dx - \int V_z v_{c,x}\theta dx
\end{aligned}
\tag{14}
$$

Obviously, Eq. (13) reduces to Eq. (14) in case of uniform members.

In references (Boissonnade 2002) and (Andrade 2007), the more complex not linearized, and therefore more precise, displacement field given in Eq. (15) is used.

$$
\begin{aligned}
U &= u - y\left(v_{c,x}\cos(\theta) + w_{c,x}\sin(\theta)\right) - z\left(w_{c,x}\cos(\theta) + v_{c,x}\sin(\theta)\right) - \omega_c\theta_x \\
&+ y_c\left(v_{c,x}(\cos(\theta) - 1) + w_{c,x}\sin(\theta)\right) + z_c\left(w_{c,x}(\cos(\theta) - 1) + v_{c,x}\sin(\theta)\right) \\
&+ (y - y_c)_{,x}(1 - \cos(\theta)) + (z - z_c)_{,x}(1 - \cos(\theta)) - yz_{c,x}\sin(\theta) + zy_{c,x}\sin(\theta) \\
V &= v - (z - z_c)\sin(\theta) - (y - y_c)(1 - \cos(\theta)) \\
W &= w + (y - y_c)\sin(\theta) - (z - z_c)(1 - \cos(\theta))
\end{aligned}
\tag{15}
$$

[6] As stated in paragraph 3.1 of this article, the expression of the energy is limited to four degrees of freedom.

Developing this displacement field as shown before leads to the following expression of the internal energy:

$$\Pi_i = \frac{1}{2}\int EI_z v_{c,xx}^2 + EI_w \theta_{,xx}^2 + GI_t \theta_{,x}^2 + EI_\psi \theta_{,x}^2 + 2EI_{w\psi}\theta_{,xx}\theta_{,x} + 2EI_{y\psi} v_{c,xx}\theta_{,x} dx$$
$$+ \frac{1}{2}\int N\left(v_{c,x}^2 + r_{yz}^2\theta_{,x}^2 - 2z_c v_{c,xx}\theta\right)dx + \int M_y\left(-v_{c,xx}\theta - \beta_z\theta_{,x}^2\right)dx \quad (16)$$

Eq. (16) also accounts for the effect of the taper of the member. One notices that the linear parts of the internal energy of Eqs. (16) and (13) are identical. However, the differences in the non-linear part cannot be overseen. The non-linear part of Eq. (16) is not influenced by the taper of the member whereas in Eq. (13) an important number of additional terms arise due to the use of the linearized displacement field. As presented in Appendix A, these supplementary terms are linked to the first or to the second derivate of the function $z(x)$ with respect to x and it can be shown that their influence on the global behavior of the member is negligible. They are therefore omitted in the final expression of the internal energy of the beam. One could also notice that the shear force is present in Eq. (13) whereas it is absent in Eq. (16). Nevertheless, it appears that when developing the stiffness matrix of the beam element, the term $-M_y v_{c,xx}\theta$ of Eq. (16) corresponds to the terms $M_y v_{c,x}\theta_{,x} - V_z v_{c,x}\theta$ of Eq. (13).

If elastic restraints are present along the beam, the energy stored therein should be added to the internal potential energy. Hence, the final expression of the internal potential energy of the beam reads:

$$\Pi_i = \frac{1}{2}\int EI_z v_{c,xx}^2 + EI_w \theta_{,xx}^2 + GI_t \theta_{,x}^2 + EI_\psi \theta_{,x}^2 + 2EI_{w\psi}\theta_{,x}\theta_{,xx} + 2EI_{y\psi} v_{c,xx}\theta_{,x} dx$$
$$+ \frac{1}{2}\int N\left(v_{c,x}^2 + r_{yz}^2\theta_{,x}^2 + 2z_c v_{c,x}\theta_{,x}\right)dx + \int M_y\left(v_{c,x}\theta_{,x} - \beta_z\theta_{,x}^2\right)dx + \int V_z\left(-v_{c,x}\theta\right)dx \quad (17)$$
$$+ \frac{1}{2}\sum v_c^2 k_v + \frac{1}{2}\sum v_{c,x}^2 k_{v,x} + \frac{1}{2}\sum \theta^2 k_v + \frac{1}{2}\sum \theta_{,x}^2 k_{\theta,x}$$

where v_c is the lateral displacement at the restraint, k_v is the stiffness of the elastic restraint against lateral displacement, $v_{c,x}$ is the lateral curvature at the restraint, $k_{v,x}$ is the stiffness of the elastic restraint against lateral curvature, θ is the torsional rotation at the restraint, k_θ is the stiffness of the elastic restraint against torsional rotation, $\theta_{,x}$ is the warping deformation at the restraint, $k_{\theta,x}$ is the stiffness of the restraint against warping deformation.

3.3 The work of external loads

The work of the external loads can be determined according Eq. (3) recalled below.

$$\Pi_e = \sum\int q_z W dx + \sum F_z W \quad (3)$$

The vertical displacement W is equal to the sum of the vertical displacement of the shear center w_c and the vertical displacement of the load application point due to rotation of the member. In

accordance with the limitation to four degrees of freedom, the vertical displacement of the shear center is neglected. Therefore, the vertical displacement W can be determined according to Fig. 4.

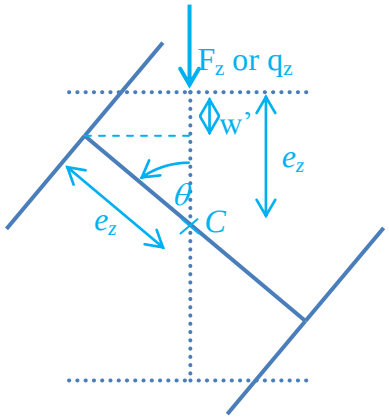

Figure 4: Member after rotation

In Fig. 4, *C* is the shear center, e_z is the distance between the shear center and the load application point and w' is the vertical displacement of the load application point due to the rotation θ. The vertical displacement w' is given in Eq. (18).

$$W = -w' = -\left(e_z - e_z \cos(\theta)\right) \tag{18}$$

Developing the cosine function as a series and stopping the development at the quadratic term, Eq. (18) becomes:

$$W = -e_z \frac{\theta}{2} \tag{19}$$

Introducing Eq. (19) into Eq. (3), the final expression of the work of the external loads is obtained:

$$\Pi_e = \sum \int q_z \left(-e_z \frac{\theta}{2}\right) dx + \sum F_z \left(-e_z \frac{\theta}{2}\right) \tag{20}$$

3.4 Transition from the potential energy of the member to the stiffness matrix of the finite element

In order to obtain the element stiffness matrix of the beam element, the 4 degrees of freedom kept in the expression of the potential energy of the beam are approximated with the help of the third degree hermitian polynomials given in (21):

$$\phi_1(x) = 1 - 3\left(\frac{x}{L}\right)^2 + 2\left(\frac{x}{L}\right)$$

$$\phi_2(x) = \frac{x}{L} - 2\left(\frac{x}{L}\right)^2 + \left(\frac{x}{L}\right)^3$$

$$\phi_3(x) = 3\left(\frac{x}{L}\right)^2 - 2\left(\frac{x}{L}\right)^3 \tag{21}$$

$$\phi_4(x) = -\left(\frac{x}{L}\right)^2 + \left(\frac{x}{L}\right)^3$$

The displacement functions used in Eq. (17) and Eq. (20) become:

$$v_c(x) = v_{c,1}\phi_1(x) + L v_{c,1x}\phi_2(x) + v_{c,2}\phi_3(x) + L v_{c,2,x}\phi_4(x)$$

$$\theta(x) = \theta_1\phi_1(x) + L\,\theta_{1,x}\phi_2(x) + \theta_2\phi_3(x) + L\,\theta_{2,x}\phi_4(x)^3$$

$$v_{c,x}(x) = \frac{\partial v_c(x)}{\partial x}$$

$$v_{c,xx}(x) = \frac{\partial^2 v_c(x)}{\partial x^2} \tag{22}$$

$$\theta_{,x}(x) = \frac{\partial \theta(x)}{\partial x}$$

$$\theta_{,xx}(x) = \frac{\partial^2 \theta(x)}{\partial x^2}$$

where L is the length of the beam element and the indexes "$_{,1,}$" and "$_{,2,}$" refer to nodes 1 and 2 of the element, respectively. The internal moment acting along a beam element is linearly approximated by Eq. (23).

$$M_y(x) = M_1\left(1 - \frac{x}{L}\right) + M_2\,\frac{x}{L} \tag{23}$$

The corresponding shear force acting along the beam element is obtained by deriving Eq. (23) with respect to x.

$$V_z = -\frac{\partial M_y(x)}{\partial x} = \frac{M_1 - M_2}{L} \tag{24}$$

Introducing Eqs. (22) to (24) into Eqs. (17) and (20) and solving the derivation of Eq. (4) lead to the element stiffness matrices implemented in *LTBeamN*.

4. Validation of *LTBeamN*

4.1 General

In the following, some numerical tests are presented in order to validate *LTBeamN*. The results of *LTBeamN* are compared to results obtained with the commercial software ANSYS based on a shell model using element Shell 281 (see Fig. 5). Kinematic conditions are applied along the member in order to prevent local and distortional buckling and interaction between the two previous modes and the global lateral torsional buckling mode. These kinematic conditions are illustrated in red on Fig. 5. The torsional rotation of each node of a given cross section is defined equal to the torsional rotation of the node situated at the shear center.

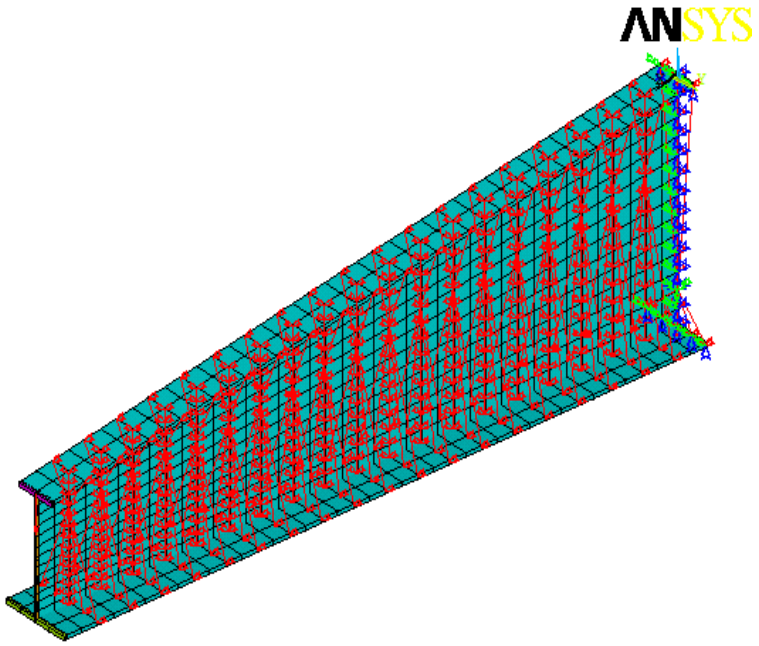

Figure 5: Finite Element model used for the validation of *LTBeamN*

In all examples, the Young's modulus of the steel is 210000 MPa and the Poisson's ratio is equal to 0,3. In order to highlight the influence of the tapered web the results obtained on the basis of the energy expression given in Eq. (14) are also shown (non-tapered beam element). Some of the examples shown next are also used in references (Andrade 2007) and (Asgarian 2013) to validate their respective approach.

4.2 Example #1

In this first example, the clamped beam of Fig. 6 is studied. The load is applied on the upper flange at the free end. The critical load is calculated for both types of cross section geometries shown in Fig. 6.

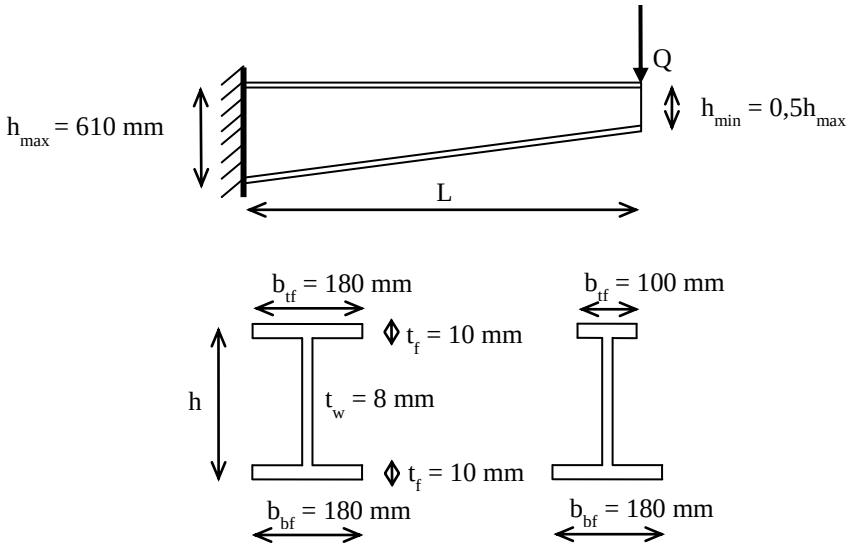

Figure 6: Example #1

Table 1 gives the results in case of the double-symmetric section.

Table 1: Critical loads for the double-symmetric section

Length [m]	Reference (kN)	LTBeamN (kN)	Difference with respect to the reference (%)	Non-tapered beam element (kN)	Difference with respect to the reference (%)
2	173,3	176,5	-1,81	355,2	-51,21
4	44,55	45,10	-1,22	62,74	-28,99
6	22,69	22,83	-0,61	26,21	-13,43
8	13,95	13,97	-0,14	14,71	-5,17
10	9,31	9,30	0,11	9,44	-1,38

Table 2 gives the results in case of the mono-symmetric section.

Table 2: Critical loads for the mono-symmetric section

Length [m]	Reference (kN)	LTBeamN (kN)	Difference with respect to the reference (%)	Non-tapered beam element (kN)	Difference with respect to the reference (%)
2	77,21	76,24	1,27	130,7	-40,93
4	26,76	26,78	-0,07	32,43	-17,48
6	15,08	15,03	0,33	16,20	-6,91
8	9,680	9,623	0,62	9,917	-2,39
10	6,610	6,563	0,76	6,642	-0,48

The influence of the taper of the beam can easily be identified regarding Tables 1 and 2. Especially for short, i.e. for highly tapered beams, the beam element based on the energy expression of Eq. (24) gives poor results compared to the reference. *LTBeamN*, however, gives results that are very close to the reference.

4.3 Example #2

In example 2, a clamped member subjected to a vertical load, applied at the upper flange at its free end, and a compression force is studied. The ratio of the axial force to the vertical force is varied. As shown in Fig. 7, the beam possesses a double-symmetric section; the results are given in table 3.

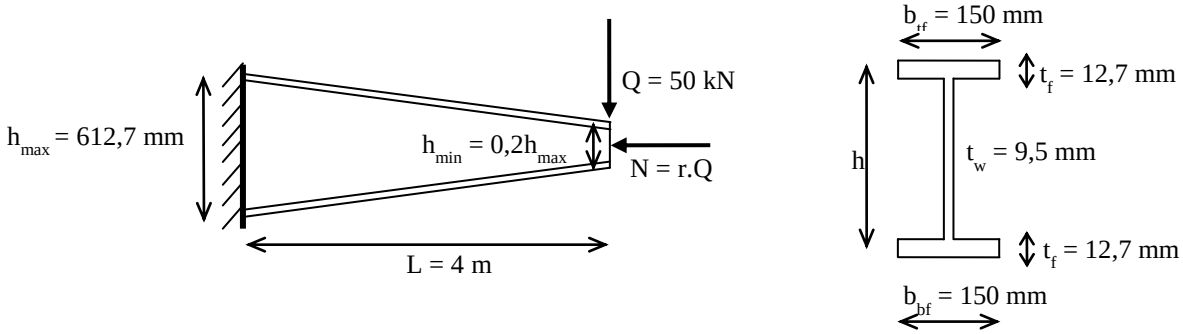

Figure 7: Example #2

Table 3: Critical load amplification factors for the double-symmetric section

Ratio r =N/Q	Reference	LTBeamN	Difference with respect to the reference (%)	Non-tapered beam element	Difference with respect to the reference (%)
0	1,979	1,943	1,85	1,851	6,92
1	1,742	1,722	1,16	1,642	6,09
2	1,475	1,469	0,41	1,411	4,54
4	1,006	1,010	-0,40	0,991	1,54

As for example 1 the results obtained with *LTBeamN* are very close to the reference whereas non tapered beam elements show non negligible differences to the reference results.

4.4 Example #3

A rather non-conventional beam is used to validate *LTBeamN* for special cases. The beam is shown in Fig. 8. This example is about a double tapered beam with a load applied on the upper flange. The sections along the beam are aligned at their centroid.

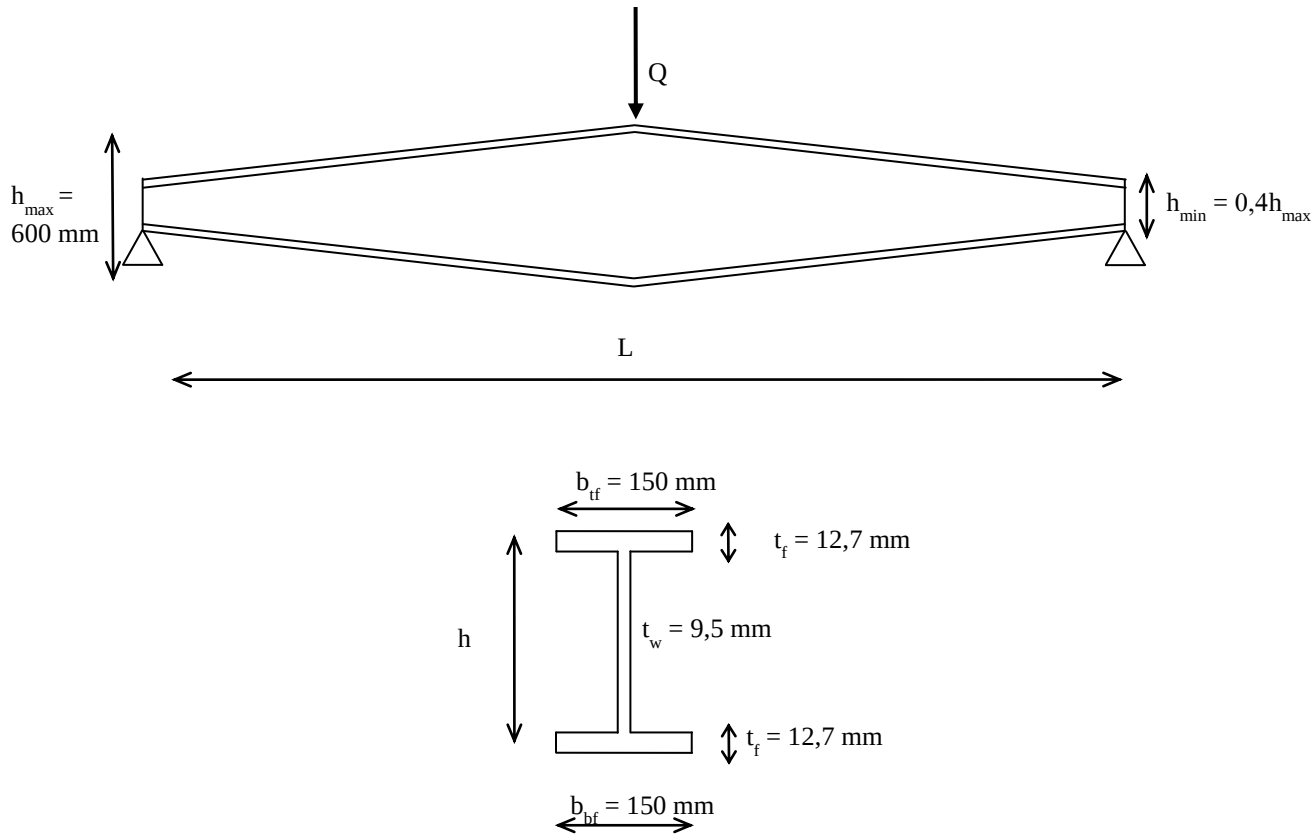

Figure 8: Example #3

Table 4: Critical loads

Length [m]	Reference (kN)	LTBeamN (kN)	Difference with respect to the reference (%)	Non-tapered beam element (kN)	Difference with respect to the reference (%)
6	63,58	62,17	2,27	81,33	-21,82
9	30,55	29,97	1,94	33,66	-9,24
12	18,05	17,76	1,63	18,80	-3,99

It can be seen that even for this extreme situation *LTBeamN* yields very good results.

4.5 Example #4

The fourth example, not included in the given references, is a modification of the previous one. Instead of the double-symmetric cross section, a mono-symmetric one is used. The sections along the beam are aligned at their centroids so that a discontinuity in the curve linking the shear centers of the sections is created. In order to illustrate this fact, this curve is schematically illustrated by the doted blue line in Fig. 9.

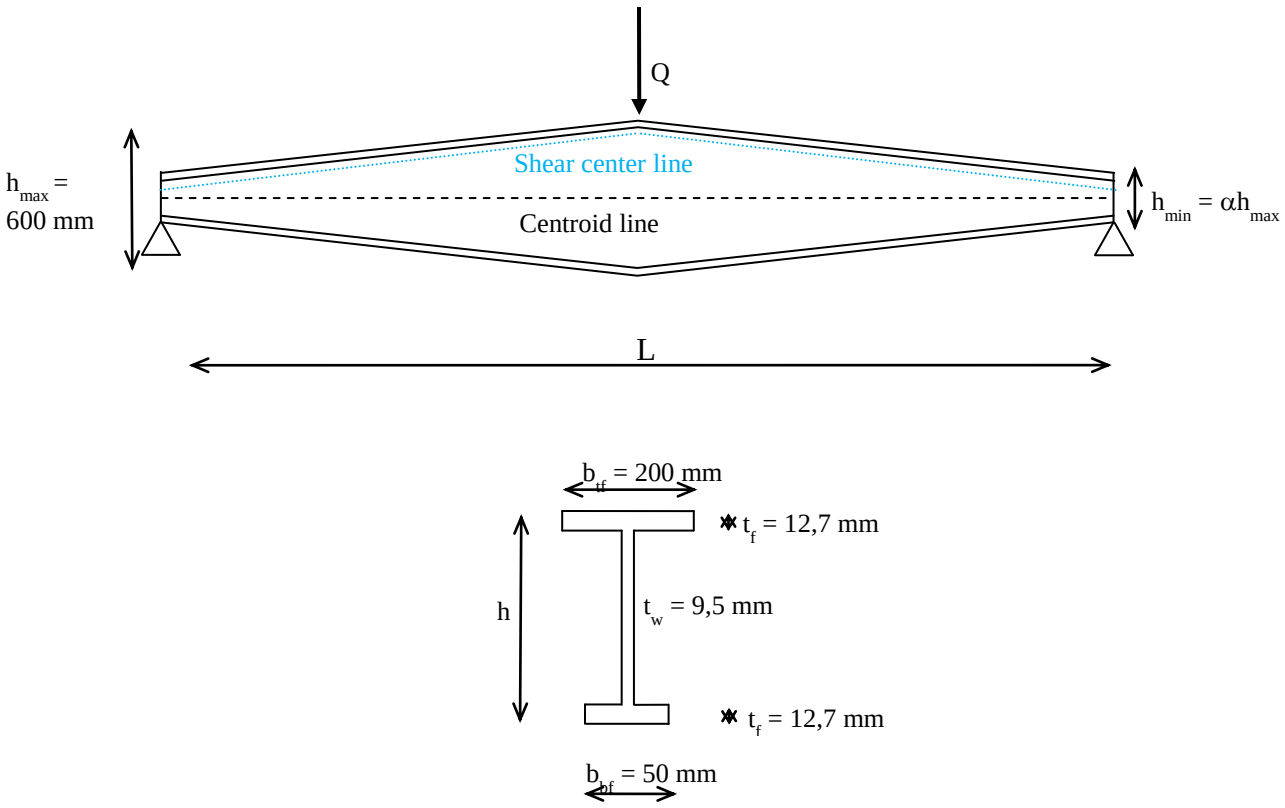

Figure 9: Example #4

Owing to this discontinuity, the curve linking the shear centers of consecutive sections does not correspond to the center of torsional twist, i.e. the curve of zero lateral displacement when pure torsion is applied to the beam. Fig. 10 shows results of Finite Element analysis of the beam of Fig. 9 with a length of 4,5 m subjected to a torsional moment at mid-span only. In Fig. 10 the lateral displacement is given. For the ease of representation only the zone of near zero lateral displacement (at the proximity of the center of torsional twist, called torsion center hereafter) is colored. For this case, it can be seen that torsion center can be well **approximated** by a straight line passing through the shear centers of the sections at the supports, i.e. the sections rigidly restrained against rotation about the longitudinal axis. Once again the shear center line is plotted on Fig. 10.

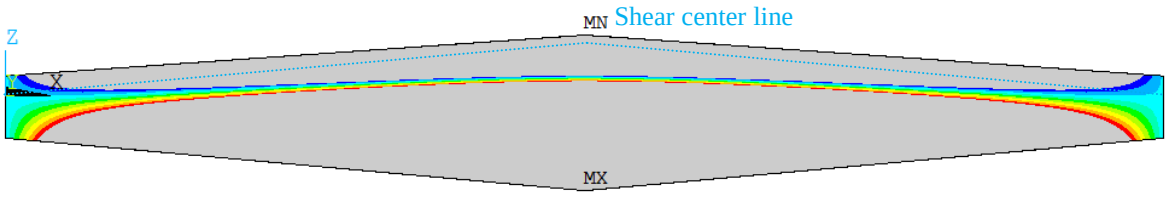

Figure 10: Lateral displacement of the beam of Fig.9 subjected to a torsional moment at mid-span only

In §3.2 of this paper, it has been supposed implicitly that the shear center coincides with the torsion center. In Fig. 10 one sees that this is not true anymore. Consequently, the distance used to evaluate the stabilizing or destabilizing effect of a vertical load should not be evaluated with reference to the shear center but with reference to the real **t**orsion **c**enter. When the distance e_z is

defined with respect to this axis, *LTBeamN* gives the results shown in the third column of table 5 (e_z^{TC} is the distance between the load application point ant the torsion center line). Otherwise, if the distance e_z is defined with respect to the **s**hear **c**enter of the section, the results of the fifth column are obtained.

Table 5: Critical loads

Length [m]	Reference (kN)	LTBeamN e_z^{TC} (kN)	Difference with respect to the reference (%)	LTBeamN e_z^{SC} (kN)	Difference with respect to the reference (%)
6	85,09	83,73	1,62	57,94	46,86
9	39,27	38,71	1,45	29,71	32,18
12	22,47	22,18	1,31	18,14	23,87

Regarding Table 5, the influence of the distance e_z is obvious. Defining e_z as the distance between the load application point and the torsion center line leads to rather satisfactory results even for the extreme case shown in Fig. 9, whereas taking the distance e_z as the distance between the shear center and the load application point gives results far away from the reference.

4.6 Example #5

The last example presented here is similar to the two previous ones. The beam of example 3 is studied again. In this example the sections are aligned at the upper flange so that, once again, the shear center line possesses a discontinuity at mid span. The load is applied at the shear center. The results are given in Table 6.

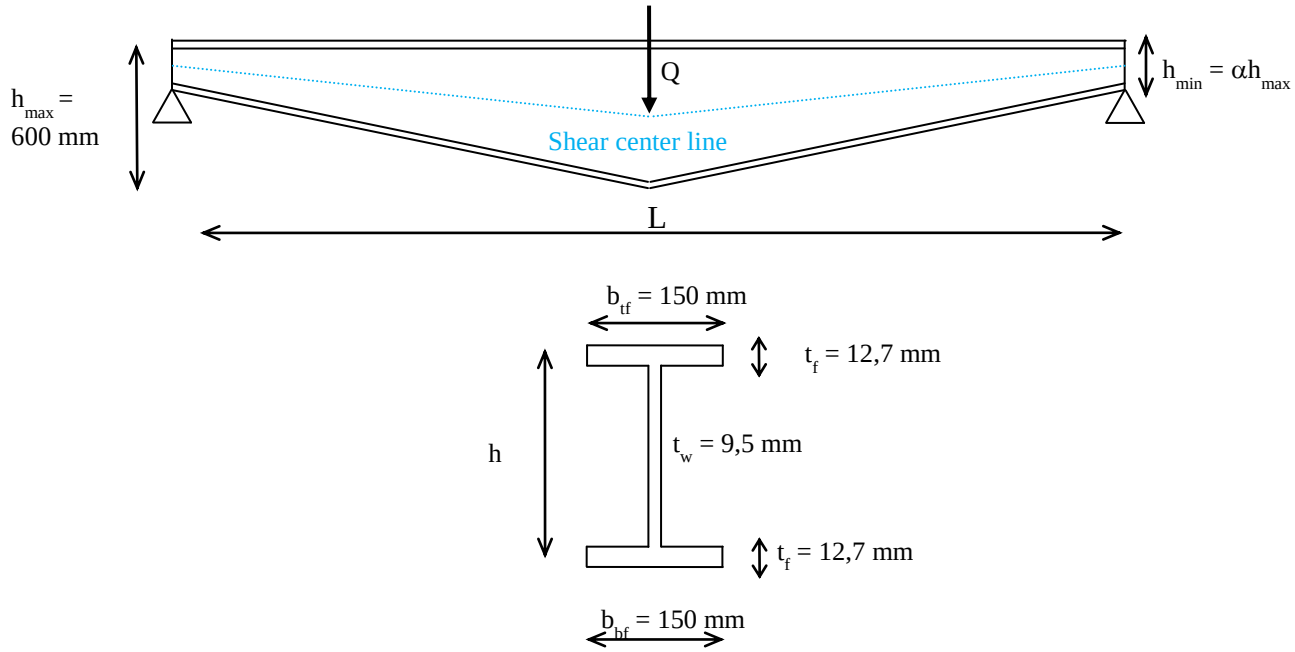

Figure 11: Example #5

Table 6: Critical load

Length [m]	Reference (kN)	LTBeamN e_z^{TC} (kN)	Difference with respect to the reference (%)	LTBeamN e_z^{SC} (kN)	Difference with respect to the reference (%)
6	146,4	147,5	-0,75	193,7	-24,42
9	56,20	56,25	-0,09	69,32	-18,93
12	29,23	29,19	0,14	34,55	-15,40

This example also shows that defining e_z as the distance between the load application point and the torsion center line yields very good results.

5. Application of *LTBeamN* for the design of non-uniform members with lateral restraints

5.1 Description of the example

In the following, it is shown how *LTBeamN* facilitates the design of non-uniform members with lateral restraints. Members in these situations are rather usual in industrial steel buildings, in columns and rafters of portal frames, for example. Even if non-uniform members are widely used, the interaction formulas proposed in most standards are based on studies of uniform members without intermediate lateral restraints. Therefore, their application to other cases is questionable. European standard "Eurcode 3 part 1-1" proposes a "general method for lateral and lateral torsional buckling of structural components". In the following this method, presented in (Müller 2003) is used for the design of the non-uniform steel column of Fig. 12. The studied column is fully restrained against lateral displacement and torsional rotation at its origin, its extremity and at a height of 6 m. In addition, it possesses a lateral restraint at its outer flange at a height of 3 m. The column is subjected to an axial force and a bending moment at its upper extremity and a uniformly distributed load of 6 kN/m acting outwards on the outer flange.

5.2 Design procedure

As stated earlier, the design is based on the calculation of two parameters: the critical load amplification factor $\alpha_{cr,op}$ and the ultimate load amplification factor for the in plane behavior of the member $\alpha_{ult,k}$. This last factor should account for in-plane second order effects and relevant imperfections. It can be calculated using a standard design formula for in-plane buckling (so that the 2nd order effects and imperfections are accounted for by the buckling reduction factor and the axial force bending moment interaction factor) or directly through a second order calculation of the member. Here, the second option is used and the internal forces in the member are determined by means of a second order analysis of the beam including a half wave sinusoidal imperfection with an amplitude of 3,6 cm (=L/250) according to (CEN 2005). The obtained design internal forces are plotted on Fig. 13.

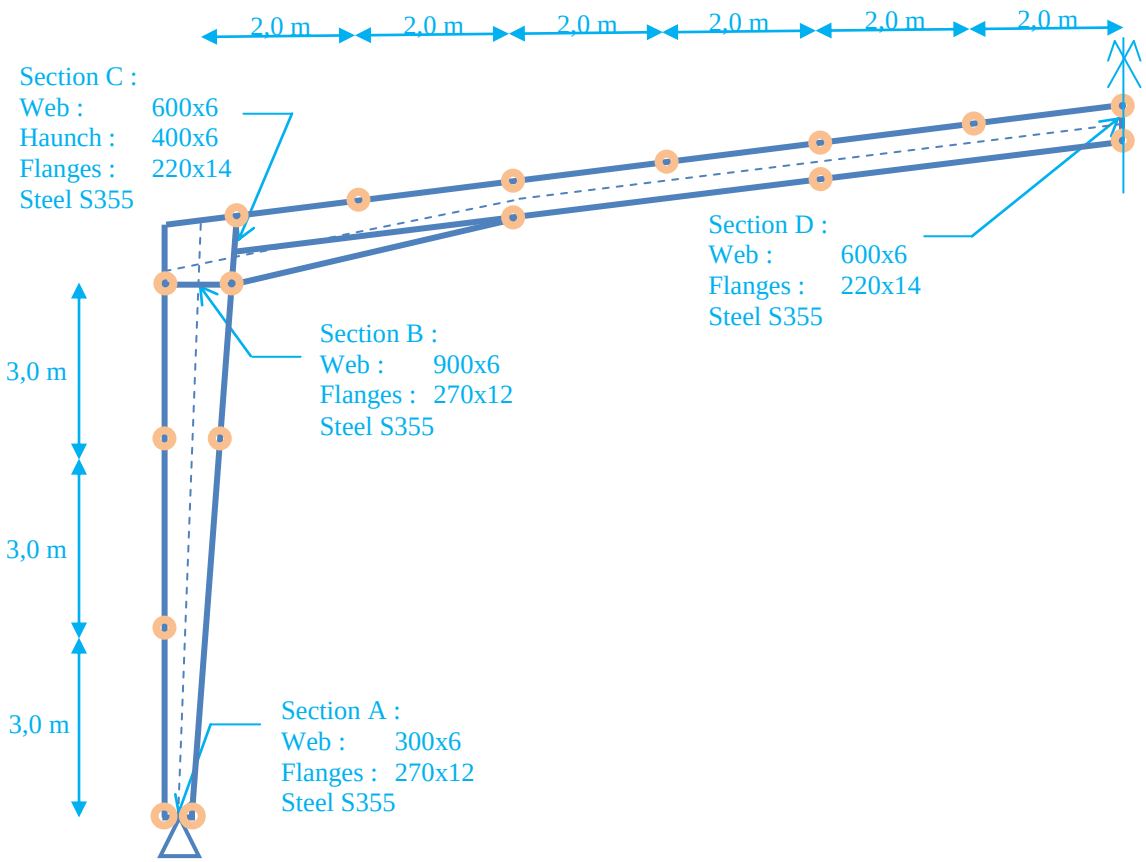

Figure 12: Portal frame with non-uniform column and haunched rafter

For sake of simplicity, the evolution of the factor $\alpha_{ult,k}$ is now calculated assuming that the sections are semi-compact and can develop their full elastic bending capacity. However, the sections at the upper end of the column are slender according to (CEN 2005); a reduction of the axial and the bending capacity due to local buckling effects should therefore be made. Fig. 14 shows the evolution of the factor $\alpha_{ult,k}$.

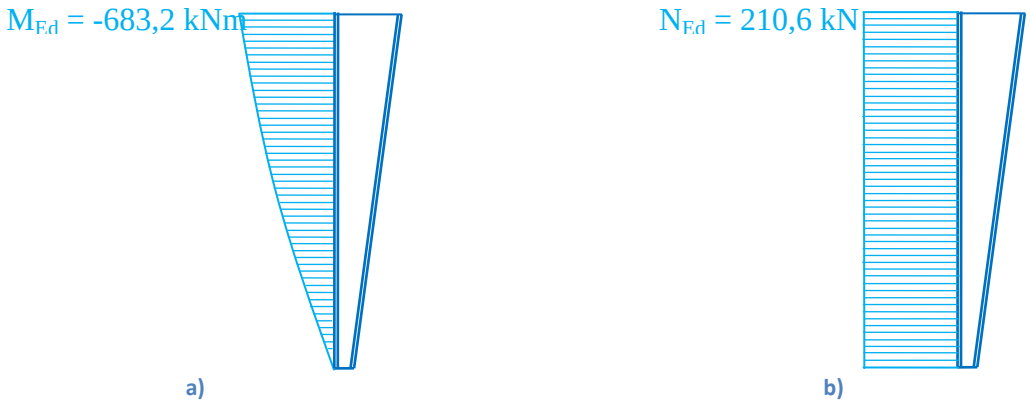

Figure 13: a) Design bending moment and b) axial force

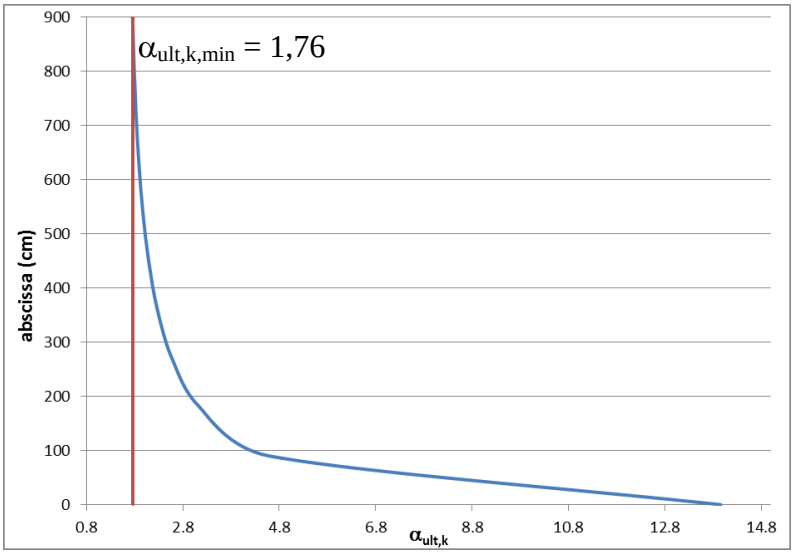

Figure 14: Evolution of the ultimate load amplification factor for in-plane behavior

The critical load amplification factor for out-of-plane buckling is calculated with *LTBeamN*. The eigen-mode obtained is shown in Fig. 15. The corresponding value of the critical load amplification factor is 2,97.

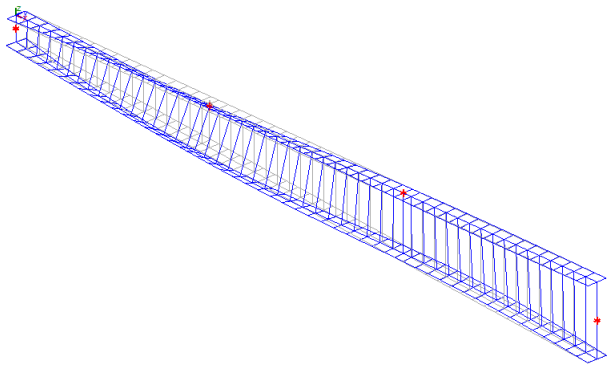

Figure 15: 1st eigen-mode of the column

The overall out-of-plane slenderness can now be calculated according to Eq. (25):

$$\bar{\lambda}_{op} = \sqrt{\frac{\alpha_{ult,k}}{\alpha_{cr,op}}} = \sqrt{\frac{1{,}76}{2{,}97}} = 0{,}77 \tag{25}$$

The overall reduction factor χ_{ov} is calculated with Eqs. (26) and (27):

$$\phi = 0{,}5\left(1 + \alpha\left(\bar{\lambda}_{op} - 0{,}2\right) + \bar{\lambda}_{op}^2\right) = 0{,}5\left(1 + 0{,}76\left(0{,}77 - 0{,}2\right) + 0{,}77^2\right) = 1{,}013 \tag{26}$$

$$\chi_{ov} = \frac{1}{\phi + \sqrt{\phi^2 - \bar{\lambda}_{op}^2}} = \frac{1}{1{,}013 + \sqrt{1{,}013^2 - 0{,}77^2}} = 0{,}598 \tag{27}$$

The design of the column can be considered appropriate if the criterion of Eq. (28) is fulfilled:

$$\frac{\chi_{ov}\alpha_{ult,k}}{\gamma_{M1}} \geq 1{,}0 \tag{28}$$

where γ_{M1} is the partial (safety) factor. For the column of this example the criterion reads:

$$\frac{0{,}598 \times 1{,}76}{1{,}0} = 1{,}05 \geq 1{,}0 \tag{29}$$

The criterion is satisfied.

6. Conclusions

This paper has presented the development of a finite beam element used for the calculation of the critical load for out-of-plane instability. It accounts for the influence of axial forces and in-plane bending moments, the non-uniformity of the member and lateral restraints. It has been shown that the taper of a member greatly influences its behavior, i.e. additional cross section parameters arise from the taper and have to be considered in the linear stiffness matrix of the element. Moreover, in cases of members whose shear center line possesses a discontinuity, it has been demonstrated that the distance influencing the stabilizing or destabilizing effect of vertical loads should not be calculated with reference to the shear center but rather with reference to the line passing through two consecutive torsionally restrained sections.

The developed finite beam element has been implemented in the freely downloadable program *LTBeamN*. This program can be used to facilitate the design of non-uniform members with lateral restraints according to the "general method for lateral and lateral torsional buckling of structural components" as proposed in European standards.

References

Andrade, A., Camotim, D., Dinis, P.B. (2007). "Lateral-torsional buckling of songly symmetric web-tapered thin-walled I-beams: 1D model vs. shell FEA". Computers & Structures 85 (17-18) 1373-1359.

Asgarian, B., Soltani, M., Mohri, F. (2013). "Lateral-torsional buckling of tapered thin-walled beams with arbitrary cross-sections." Thin walled structures 62 (1) 96-108.

CEN (Comité Européen de Normalisation) (2005). "Eurocode 3: Design of Steel Structures, Part 1–1: General rules and rules for buildings (EN 1993-1-1)", Brussels.

Boissonnade, N. (2002). "Mise au point d'un élément fini de type poutre a section variable et autres applications à la construction métallique. " Ph.D thesis (in French).

Bradford, M.A. (1988). "Stability of tapered I-beams." Journal of Constructional Steel Research 9 (3) 195-206.

Galéa, Y, (2003). "Elastic critical lateral torsional buckling moment of beams – Presentation of LTBeam." (in French) Revue Construction Métallique (2) 47-76.

Kitipornchai, S., Dux, P.E. (1982). "Elastic buckling of laterally continuous I-beams." Journal of the structural division 108(9) 2099-2116

Kitipornchai, S., Trahair, N.S. (1972). "Elastic stability of tapered I-beams." Journal of the Structural Division 98 (3) 713-728.

Kitipornchai, S., Trahair, N.S. (1975). "Elastic stability of tapered monosymmetric I-beams." Journal of the Structural Division 101 (8) 1661-1678

LTBeamN, program for the calculation of the critical load amplification factor for uniform and non-uniform members with or without intermediate lateral restraints and complex boundary conditions, freely downloadable on: https://www.cticm.com/content/logiciels

Müller, Chr. (2003). "Zum Nachweis ebener Tragwerke aus Stahl gegen seitliches Ausweichen" (in German), Ph.D thesis.

Nethercot, D.A., Trahair, N.S. (1976). "Lateral buckling approximation for elastic beams". The structional engineer 54 (6) 197-204.

Ronagh, H.R., Bradford M.A., Attard, M.M. (2000). "Nonlinear analysis of thin-walled members of variable cross-section. Part I: Theory." Computers & Structures 77 (3).

Wilde, P. (1968). "The torsion of thin-walled bars with variable cross-sections." Archiwum Mechaniki Stosowanej 4 (20) 431-443.

Appendix A

$$I_{\psi} = \int 4\omega_{c,x}^2 dA \tag{A-1}$$

$$I_{\omega\psi} = \int 2\omega_c \omega_{c,x} dA \tag{A-2}$$

$$I_{y\psi} = \int 2y\omega_{c,x} dA \tag{A-3}$$

$$\xi_{z.zx} = \frac{1}{I_y}\int z(z_{,x} - z_{c,x}) dA \tag{A-4}$$

$$\beta_{z,x} = \frac{1}{I_y}\int z\left((z_{,x} - z_{c,x})(z - z_c) + (y_{,x} - y_{c,x})(y - y_c)\right) dA \tag{A-5}$$

$$\beta_{z,x2} = \frac{1}{2I_y}\int z\left((z_{,x} - z_{c,x})^2 + (y_{,x} - y_{c,x})^2\right) dA \tag{A-6}$$

$$r_{z,x} = \int (z_x - z_{c,x}) dA \tag{A-7}$$

$$r_{yz,x}^2 = \frac{1}{A}\int \left((z_{,x} - z_{c,x})(z - z_{c,}) + (y_{,x} - y_{c,x})(y - y_{c,})\right) dA \tag{A-8}$$

$$r_{yz,x2}^2 = \frac{1}{A}\int \left((z_{,x} - z_{c,x})^2 + (y_{,x} - y_{c,x})^2\right) dA \tag{A-9}$$